Cardiology Research and Cardiovascular Medicine
Pratt RD, et al. Cardiolog Res Cardiovasc Med 10: 281.
www.doi.org/10.29011/2575-7083.100281
www.gavinpublishers.com

OPEN ACCESS

GAVIN PUBLISHERS

Research Article

The Adipocyte Na/K-Atpase Oxidant Amplification Loop is the Central Regulator of Western Diet-Induced Obesity and Associated Comorbidities

Rebecca D Pratt, Cameron Brickman, Athar Nawab, Cameron Cottrill, Brian Snoad, Hari Vishal Lakhani, Juan R Sanabria, Zijian Xie, Joseph I Shapiro, Komal Sodhi, Jiang Liu*

Departments of Medicine, Surgery, Biomedical Sciences, and Healthcare Informatics Program, Joan C. Edwards School of Medicine, Marshall University, USA

***Corresponding author:** Jiang Liu, Associate Professor of Surgery and Biomedical Sciences, Marshall University Joan C Edwards School of Medicine, WV 25701, USA

Citation: Pratt RD, Brickman C, Nawab A, Cottrill C, Snoad B, et al. (2025) The Adipocyte Na/K-Atpase Oxidant Amplification Loop is the Central Regulator of Western Diet-Induced Obesity and Associated Comorbidities. Cardiol Res Cardio vasc Med 10:281. DOI:https://doi.org/10.29011/2575-7083.100281

Received Date: 02 April, 2025; **Accepted Date:** 09 April, 2025; **Published Date:** 14 April, 2025

Abstract

Obesity has become a worldwide epidemic. We have previously reported that systemic administration of pNaKtide which targets the Na/K-ATPase oxidant amplification loop (NKAL) was able to decrease systemic oxidative stress in mice. As adipocytes are believed to play a central role in the development of oxidative stress and its related comorbidities, we examined whether lentiviral-mediated adipocyte-specific expression of NaKtide, a peptide derived from the N domain of the Na/K-ATPase α1 subunit, could ameliorate the effects of the WD. C57BL/6 mice were fed a WD, which activated Na/K-ATPase signaling in the adipocytes and induced an obese phenotype, causing increases in plasma levels of leptin, IL-6, and TNFα. WD also showed decreased locomotor activity and downregulated tyrosine hydroxylase in brain tissue, but increased markers of neurodegeneration and neuronal apoptosis. Lentiviral-mediated adipocyte-specific expression of NaKtide in mice fed a WD attenuated all these changes including the brain biochemical alterations and behavioral adaptations. These data suggest that adipocyte-derived cytokines play an essential role in the development of obesity induced by a WD and that targeting the adipocyte NKAL loop may serve as an effective therapeutic strategy.

Keywords: NaKtide, obesity, lentivirus, Na/K-ATPase signaling, ROS, adipocyte

Main Text

Obesity is a major worldwide health challenge as it is often associated with other comorbidities including (but not limited to) metabolic syndrome, cardiovascular diseases, chronic kidney disease, non-alcoholic steatohepatitis (NASH), and neurodegenerative disorders [1]. It is estimated that by the year 2030, 38% of the world's adult population will be overweight and 20% will be obese [2]. Although traditionally the adipocyte had been thought to play a passive role in the process of obesity development, recent studies have established adipocyte malfunction as playing a causative role in the pathogenesis of obesity, associated systemic oxidant stress, and the comorbidities of obesity including insulin resistance, accelerated cardiovascular disease and NASH [2,3]. Evidence also suggests that deranged mitochondrial function and chronic inflammation in the adipocytes contribute to the pathogenesis of obesity [3, 4].

Our group has demonstrated that the Na/K-ATPase functions as a scaffolding protein, affecting a signal cascade that also serves

to amplify oxidants in a feed-forward manner [5-15]. This Na/K-ATPase signaling function has been demonstrated in renal and cardiac tissues [16-18]. Specifically, we have demonstrated that reactive oxygen species (ROS) can both activate this Na/K-ATPase signal cascade as well as generate additional ROS through downstream consequences of this pathway [19, 20]. NaKtide, a specific peptide antagonist of Src kinase, was derived from the α1 subunit of the NaK-ATPase, consisting of Ser 415 to Gln 434 (P05023, AT1A1_HUMAN, www.uniprot.org). NaKtide or a cell permeant derivative, pNaKtide which was created by merging NaKtide with a 13 amino acid TAT leading sequence, prevents the activation of Src which is normally regulated by the α1 subunit of the Na/K-ATPase [16, 21]. Since we have demonstrated that systemic administration of pNaKtide was able to reduce oxidative stress [16], we were interested in using this molecular strategy to examine the specific tissues involved in the pathogenesis of obesity.

Lentiviral vectors have evolved over the last decade as a promising approach to target a gene of interest using a specific promoter for a specific cell type, which has been safe and highly effective in experimental models [22-25]. This strategy was chosen to test the hypothesis that adipocyte oxidant stress caused by activation of adipocyte Na/K-ATPase signaling might play a central role in the development and maintenance of obesity and its associated comorbidities.

Results

Effect of lenti-adiponectin-GFP-NaKtide on adiposity, metabolic balance, and locomotion in mice fed a WD

Since adiponectin is expressed specifically in adipocytes, the lentiviral construct with NaKtide driven by an adiponectin promoter (lenti-adiponectin-GFP-NaKtide) was used to achieve NaKtide expression specifically in adipocytes. Another lentiviral construct, the same as above but without NaKtide integration, also driven by an adiponectin promoter (lenti-adiponectin-GFP) was used as a vector control. Compared to mice fed a normal chow, mice fed a high fat and fructose supplemented western diet (WD) for 12 weeks exhibited significant increases in body weight, visceral fat, subcutaneous fat, liver weight, and heart weight, which were significantly attenuated by the transduction of lenti-adiponectin-GFP-NaKtide but not by lenti-adiponectin-GFP control vector expression (Figure 1A and Table 1). While food intake and energy intake did not differ amongst the different experimental groups (Figure 1B and C), there was a significant reduction in the energy expenditure (measured as heat production rate in unit of kcal/kg/hr) in mice fed a WD compared to control group, which was significantly ameliorated with lenti-adiponectin-GFP-NaKtide treatment (Figure 1D). Furthermore, the oxygen consumption in mice fed a WD alone (2491±149 mL/kg/hr) was also significantly decreased as compared to mice fed a normal diet (3104±88 mL/kg/hr), and treatment with lenti-adiponectin-GFP-NaKtide (3146±232 mL/kg/hr) significantly improved the oxygen consumption as compared to WD alone (n=8 per group). In agreement with the observation that obesity has been associated with decreased locomotion [26], mice fed a WD showed decreased locomotion, which was normalized by the lenti-adiponectin-GFP-NaKtide treatment (Figure 1E).

Citation: Pratt RD, Brickman C, Nawab A, Cottrill C, Snoad B, et al. (2025) The Adipocyte Na/K-Atpase Oxidant Amplification Loop is the Central Regulator of Western Diet-Induced Obesity and Associated Comorbidities. Cardiol Res Cardio vasc Med 10:281. DOI:https://doi.org/10.29011/2575-7083.100281

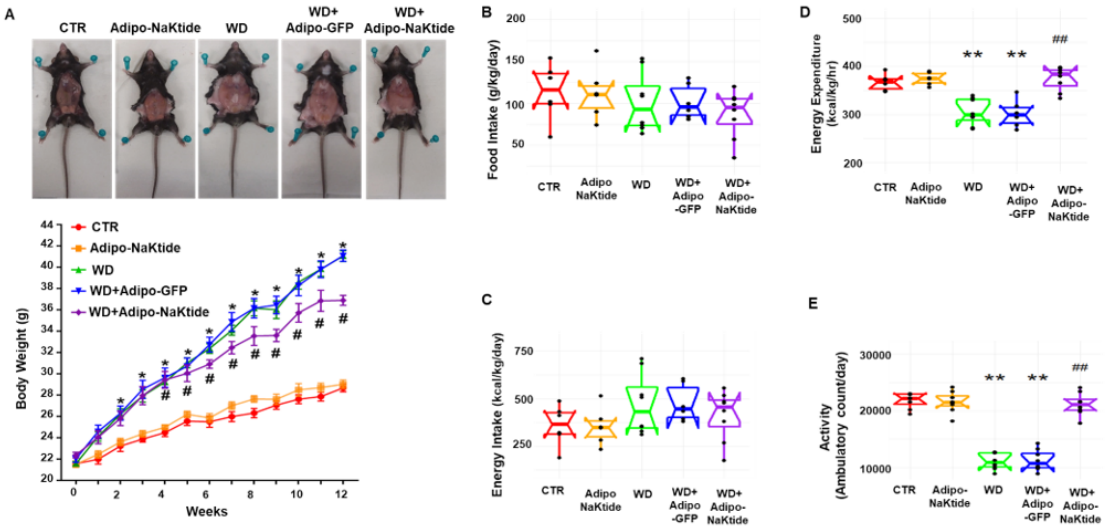

Figure 1: Effect of lenti-adiponectin-GFP-NaKtide on adiposity, metabolic balance, and locomotion in C57BL6 mice fed a WD. Body weight (Figure 1A, n=13-18 per group), food intake (Figure 1B, n=6-8 per group), energy intake (Figure 1C, n=6-8 per group), energy expenditure (Figure 1D, n=6-8 per group), and locomotion (Figure 1E, n=8 per group)) determined via CLAMS cages after 48 hours. Data are displayed as "scatter plots" showing data points and "box plots" showing the distribution of a continuous variable as described in the Methods section. $^{**}p<0.01$ vs. CTR, $^{\#\#}p<0.01$ vs. WD.

	CTR (n=18)	Adipo-NaKtide (n=13)	WD (n=17)	WD+Adipo-GFP (n=14)	WD+Adipo-NaKtide (n=18)
Visceral Fat (g)	0.36±0.03	0.39±0.04	3.06±0.08**	3.10± 0.10**	1.65± 0.09**##
Subcutaneous Fat (g)	0.10±0.02	0.14±0.02	1.64±0.06**	1.61± 0.07**	0.52± 0.05**##
Liver (g)	1.57±0.04	1.34±0.05	2.90±0.15**	3.00± 0.16**	1.98± 0.08*##
Heart (g)	0.15±0.01	0.14±0.01	0.19±0.01*	0.17± 0.01*	0.15± 0.01#

Tissue weights of visceral fat, subcutaneous fat, liver, and heart. Results are means ± SEM, n = 13-18/group. $^{*}p<0.05$, $^{**}p<0.01$ vs. control; $^{\#}<0.05$, $^{\#\#}p<0.01$ vs WD.

Table 1: Effect of lenti-adipo-NaKtide on tissue weights.

Effect of lenti-adiponectin-GFP-NaKtide on adipocyte phenotype and systemic inflammatory profile in mice fed a WD

The WD altered the morphological phenotype of visceral adipocytes with profound increases in the size and fat content of these cells. Mice treated with the lenti-adiponectin-GFP-NaKtide showed an improved adipocyte phenotype as evidenced by significantly increased numbers of adipocyte, but significant decreases in adipocyte cell area, when compared to mice fed a WD alone (Figure 2A, B & C). Mice fed a normal diet, with or without lenti-adiponectin-GFP-NaKtide treatment, showed no significant difference in aforementioned measurements. Compared to mice fed a WD alone, there was also no significant difference noted in mice fed a WD treated with the vector control (lenti-adiponectin-GFP), the lenti-adiponectin-GFP lacking the NaKtide sequence.

We next evaluated the markers directly tied to the altered adipocyte phenotype that plays a causal role in the aggravation of systemic oxidative stress. Mice fed a WD showed upregulated expression of lipogenic marker, fatty acid synthase (FAS), as well as adipogenic markers, peroxisome proliferator-activated receptor gamma (PPARγ) and mesoderm specific transcript gene (MEST), which were significantly attenuated with treatment of lenti-adiponectin-GFP-NaKtide (Figure 2D-F). Since adipose mitochondria participate in energy expenditure, we measured genes of mitochondrial biogenesis in adipose tissue. Compared to mice fed a normal diet, mice fed a WD showed a significant downregulation of peroxisome proliferator-activated receptor gamma coactivator 1-alpha (PGC-1α), a major regulator of mitochondrial biogenesis, which was ameliorated by lenti-adiponectin-GFP-NaKtide treatment (Figure 2G). Similarly, the expression of genes related to mitochondrial biogenesis and the "browning" phenomenon of adipose tissue, including mitofusin (MFN) 1 and 2, and sirtuin 1 (Sirt1) were significantly downregulated in mice fed a WD, but were all significantly increased upon treatment with lenti-adiponectin-GFP-NaKtide (Table 2). Furthermore, treatment with lenti-adiponectin-GFP-NaKtide also significantly attenuated WD-induced upregulation of the inflammatory cytokine tumor necrosis factor alpha (TNFα) and adipocyte-secreted leptin in adipose tissue, which are potent inducers of ROS generation by promoting inflammation and oxidative stress [27, 28] (Table 2).

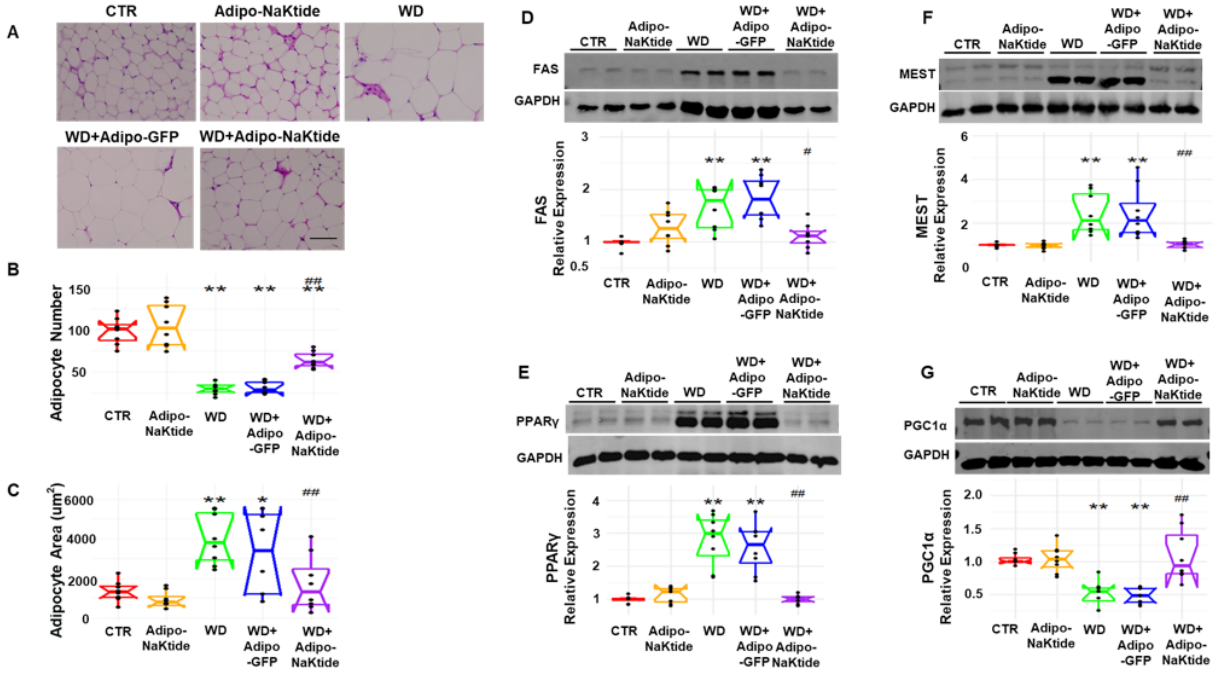

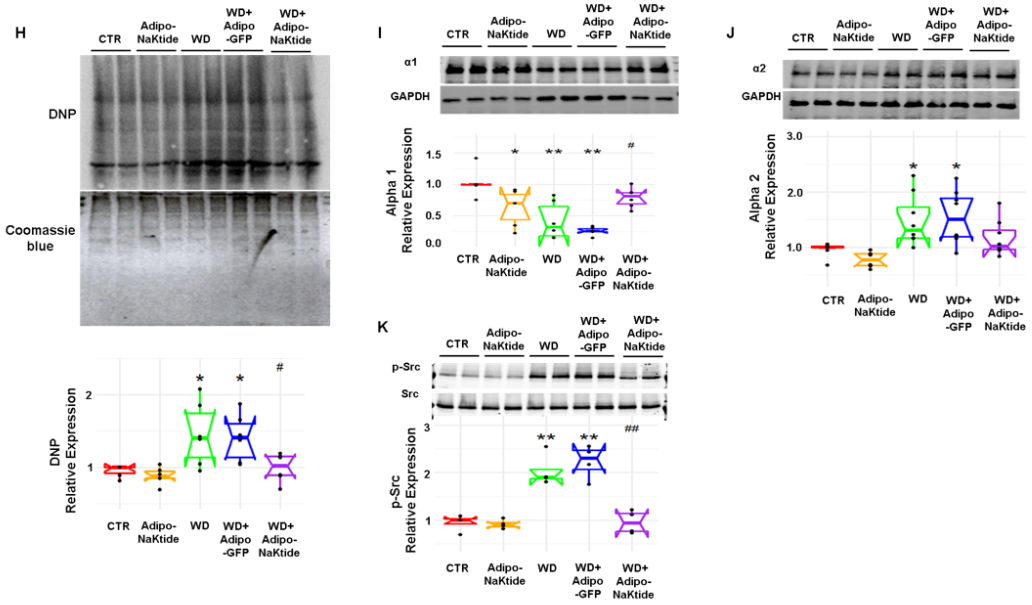

Figure 2: Effect of lenti-adiponectin-GFP-NaKtide on adipocyte phenotype, mitochondrial biogenesis, and Na/K-ATPase signaling cascade in C57BL6 mice fed a WD. Representative H&E staining in visceral adipose tissue. Images taken with 20x objective lens; scale bar represents 100 μm (Figure 2A, n=8 per group). Quantitative analysis of the adipocyte number (Figure 2B, n=8 per group) and adipocyte area (Figure 2C, n=8 per group) in visceral adipose tissue. Western blot analysis of visceral adipose tissue homogenates, with data shown as mean band density normalized to GAPDH, for fatty acid synthase (FAS) (Figure 2D, n=8 per group), peroxisome proliferator-activated receptor gamma (PPARγ) (Figure 2E, n=8 per group), mesoderm specific transcript (MEST) (Figure 2F, n=8 per group), and peroxisome proliferator-activated receptor gamma coactivator 1-alpha (PGC1α) (Figure 2G, n=8 per group). Quantitative analysis of protein carbonylation levels (shown as 2, 4-dinitrophenylhydrazine (DNP) signal) with Coomassie staining as a loading control (Figure 2H, n=6 per group). Immunoblot analysis of the α-1 subunit (Figure 2I, n=6 per group) and α-2 subunit (Figure 2J, n=8 per group) of the Na/K-ATPase, with data shown as mean band density normalized to GAPDH. phosphor-Src (p-Src) immunoblot analysis with data shown as mean band density normalized to total c-Src (Figure 2K, n=4 per group). $^{*}p<0.05$ vs. CTR, $^{**}p<0.01$ vs. CTR, $^{\#}p<0.05$ vs. WD, and $^{\#\#}p<0.01$ vs. WD.

	CTR (n=6-8)	**Adipo-NaKtide (n=6)**	**WD (n=7-9)**	**WD+Adipo-GFP (n=6-7)**	**WD+Adipo-NaKtide (n=6-7)**
MFN 1	1.02±0.07	1.27±0.16	0.27±0.11*	0.39±0.16	1.81±0.26$^{*\#\#}$
MFN 2	1.04±0.13	1.13±0.34	0.18±0.03*	0.28±0.07	1.87±0.26$^{*\#\#}$
TNFα	1.03±0.10	1.08±0.15	4.32±0.71**	4.76±0.42**	1.83±0.26$^{\#}$
Leptin	1.39±0.49	1.44±0.37	10.68±1.95*	10.78±2.05*	4.35±0.79$^{\#}$
Sirt3	1.03±0.12	1.20±0.14	0.35±0.06*	0.26±0.04*	1.49±0.22$^{\#\#}$
The relative mRNA expression of MFN 1 and 2, TNFα, leptin, and Sirt3 by RT-PCR. Results are means±SEM, n=6-9/group. $^{*}p<0.05$, $^{**}p<0.01$ vs. control; $^{\#}<0.05$, $^{\#\#}p<0.01$ vs WD.					

Table 2: Effect of lenti-adipo-NaKtide on mitochondrial and inflammatory markers in adipose tissue.

The decreased glucose tolerance in mice fed a WD was reversed by treatment with lenti-adiponectin-GFP-NaKtide (Figure 3A). Inflammatory cytokines are both indicative of high levels of oxidative stress as well as contribute to the production of oxidants. Mice fed a WD showed significantly upregulated plasma levels of the inflammatory cytokines TNFα, monocyte chemoattractant protein-1 (MCP1), and interleukin-6 (IL-6) (Figure 3B-D), as well as leptin (Figure 3E). Treatment with the lenti-adiponectin-GFP-NaKtide ameliorated the increases in the plasma concentrations of these inflammatory cytokines and leptin.

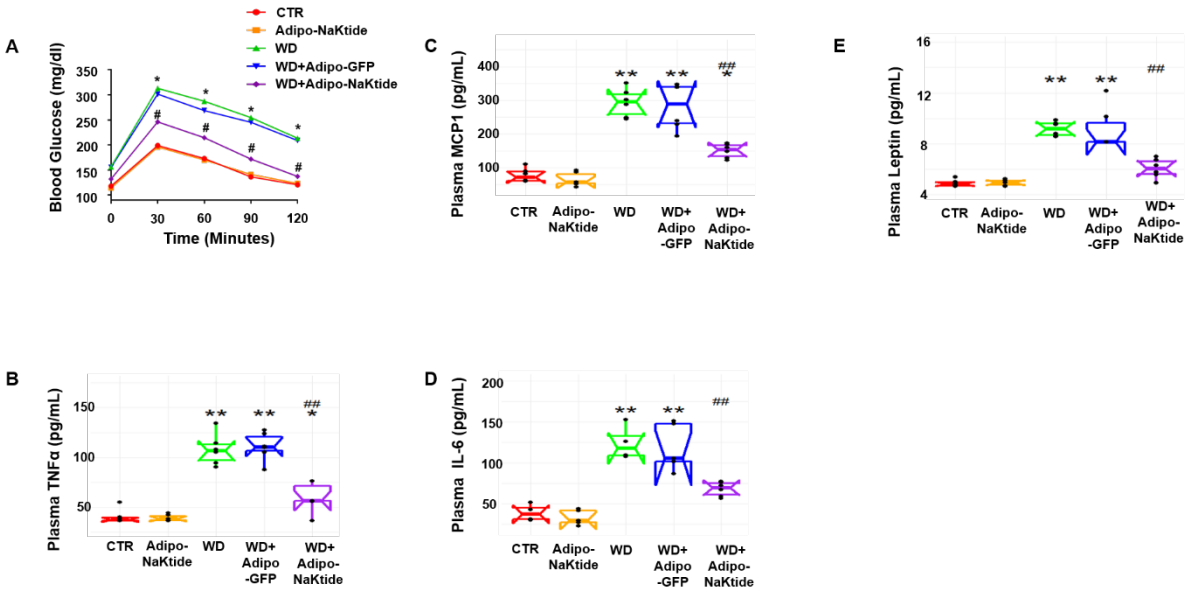

Figure 3: Effect of lenti-adiponectin-GFP-NaKtide on glucose tolerance and systemic inflammatory cytokines in C57BL6 mice fed a WD. Glucose tolerance test (Figure 3A, n=13-16 per group), Plasma levels of TNFα (Figure 3B, n=6 per group), monocyte chemoattractant protein-1 (MCP1) (Figure 3C, n=6 per group), interleukin-6 (IL-6) (Figure 3D, n=6 per group), and leptin (Figure 3E, n=6 per group) assessed by ELISA assay. $^{*}p<0.05$ vs. CTR, $^{**}p<0.01$ vs. CTR, $^{\#}p<0.05$ vs. WD, $^{\#\#}p<0.01$ vs. WD.

Effect of lenti-adiponectin-GFP-NaKtide on Na/K-ATPase/Src signaling cascade in mice fed a WD

Protein carbonylation is a well-established marker for assessing oxidative stress [29, 30]. Our results showed a significant increase in protein carbonylation in mice fed a WD, which was attenuated by treatment with the lenti-adiponectin-GFP-NaKtide (Figure 2H). WD-induced downregulation of the α1 subunit of the Na/K-ATPase and c-Src activation in visceral fat were significantly attenuated by lenti-adiponectin-GFP-NaKtide treatment (Figure 2I and 2K). However, WD-induced upregulation of the α2 subunit of the Na/K-ATPase was not significantly corrected by lenti-adiponectin-GFP-NaKtide treatment, even though with a reduced tendency was observed (Figure 2J).

Effect of lenti-adiponectin-GFP-NaKtide on neurodegeneration in mice fed a WD

Obesity and systemic oxidative stress have been implicated with neurodegenerative disorders. Tyrosine hydroxylase (TH) is a rate-limiting enzyme in the production of dopamine that was correlate with locomotor activity [31, 32]. Mice fed a WD showed significant downregulation of TH in brain tissues, which was significantly improved by lenti-adiponectin-GFP-NaKtide treatment (Figure 4A). Furthermore, in the brain tissues of mice fed a WD, there was an increase in protein carbonylation (Figure 4B), a down-regulation of postsynaptic density protein 95 (PSD95, a marker of synaptic plasticity [33] (Figure 4C), and activation of Tau (pTau/Tau ratio, a marker of tangled neuron tracks and a hallmark of neurodegenerative disease [33] (Figure 4D), which were all markedly improved by lenti-adiponectin-GFP-NaKtide treatment.

Citation: Pratt RD, Brickman C, Nawab A, Cottrill C, Snoad B, et al. (2025) The Adipocyte Na/K-Atpase Oxidant Amplification Loop is the Central Regulator of Western Diet-Induced Obesity and Associated Comorbidities. Cardiol Res Cardio vasc Med 10:281. DOI:https://doi.org/10.29011/2575-7083.100281

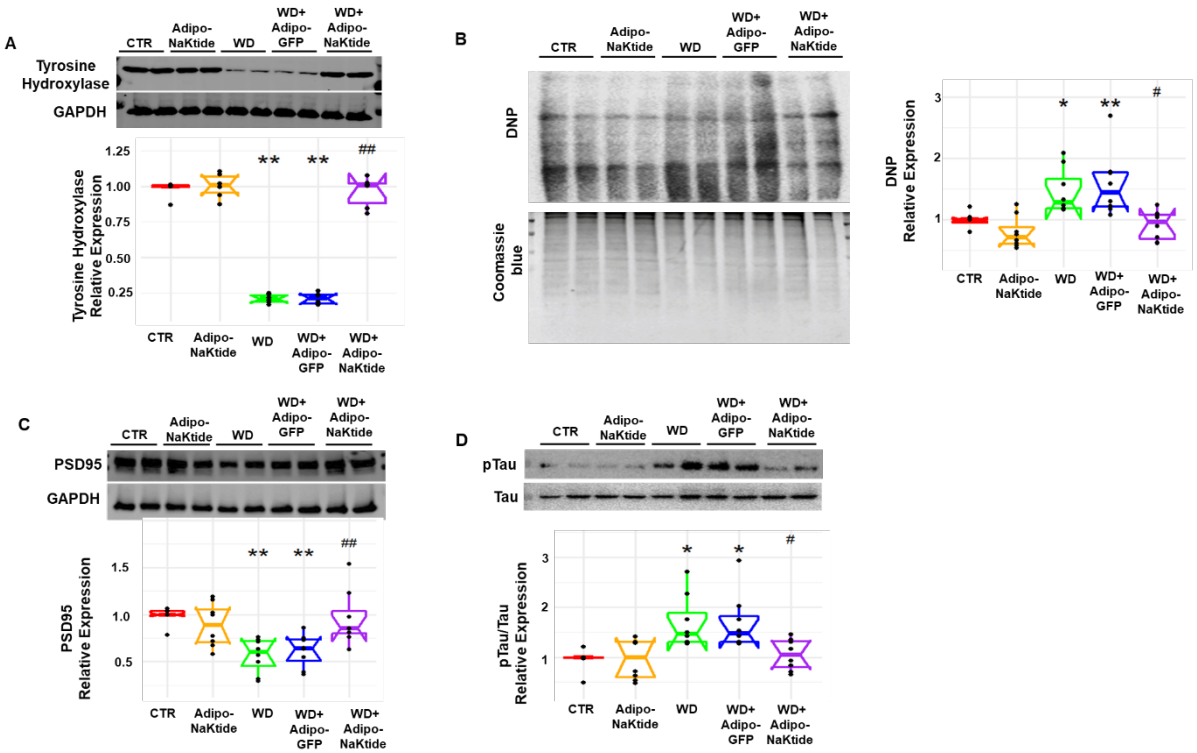

Figure 4: Effect of lenti-adiponectin-GFP-NaKtide on neurodegeneration in brain tissue in C57BL6 mice fed a WD. Immunoblot analysis for tyrosine hydroxylase (TH) (Figure 4A, n=6 per group). Protein carbonylation levels with Coomassie staining as a loading control (Figure 4B, n=8 per group). Immunoblot analysis for marker of synaptic plasticity, PSD95 (Figure 4C, n=8 per group), and marker of tangles in neuron tracks, phospho-Tau and Tau (Figure 4D, n=8 per group). $^{*}p<0.05$ vs. CTR, $^{**}p<0.01$ vs. CTR, $^{\#}p<0.05$ vs. WD, $^{\#\#}p<0.01$ vs. WD.

Discussion

In this study, we targeted the Na/K-ATPase signaling antagonist NaKtide specifically to adipocytes in mice fed a WD using a lentivirus employing adiponectin-specific promoter, to drive its expression only in adipocytes. Our results showed that targeting of NaKtide specifically to adipocytes was able to reverse WD-induced changes in metabolic profile, oxidative stress, and inflammation. This highlights the importance of the Na/K-ATPase oxidant amplification loop within the adipocyte as well as the importance of adipocyte biology itself. There is accumulating evidence suggesting that adipocyte mitochondria might play an important role in the development of dysfunctional adipocytes [34, 35]. Our results showed that PGC1α level, the master regulator of mitochondrial biogenesis and adaptive thermogenesis, was increased upon adipocyte targeted NaKtide expression. Furthermore, the expression of genes associated with mitochondrial biogenesis and "browning" of fat, including MFN1, MFN2, and SIRT1, were increased by NaKtide treatment. Adipocytes also showed increased protein carbonylation in mice fed a WD that was decreased by NaKtide treatment, indicating a reduction in oxidative stress within the adipose tissue.

Our results also showed that expression of the α1 subunit of the Na/K-ATPase was significantly downregulated in visceral fat by the WD. We have shown previously that oxidative stress can induce endocytosis of α1; we therefore propose that WD increases oxidative stress, increasing α1 endocytosis [36-38]. Some of the endocytosed α1 is recycled to the surface, while some is destroyed through endosomal and proteolytic pathways. Previous evidence has shown that ROS can accelerate the degradation of the Na/K-ATPase [39-43]. Hence, we propose that increased oxidative stress induced by WD leads to a decrease in total adipocyte α1 expression in mice fed a WD. Interestingly, expression of α2 subunit of Na/K-ATPase was noted to move in the opposite direction as α1; this may be related to a compensatory mechanism that has yet to be elucidated. Treatment with NaKtide also blocked Na/K-ATPase-regulated Src activation in mice fed a WD.

Studies in mouse models of obesity have shown that increased systemic oxidative stress is due to an altered adipocyte phenotype [44, 45]. Comorbidities such as insulin resistance and dyslipidemia also contribute to systemic oxidative stress [46]. Attenuation of the NKAL in the adipocytes, through NaKtide introduction, during exposure to the WD ameliorated oxidant stress within these cells as well as the WD-induced glucose intolerance. In particular, the increases in plasma levels of leptin and inflammatory cytokines (i.e., IL-6, TNFα, and MCP1) in mice fed a WD were dramatically attenuated by NaKtide expression in adipocytes. This suggests a central role of the Na/K-ATPase signaling loop within adipocytes in the development of obesity and systemic oxidative stress in response to a WD.

More interestingly, we observed profound changes in the locomotor activity of animals with the switch to a WD, which were dramatically attenuated by adipocyte NaKtide treatment. Specifically, animals given the WD demonstrated marked reductions in activity level and calculated energy expenditure. We found that these behavioral changes were strongly associated with changes in brain tyrosine hydroxylase expression. These changes appeared to be linked to adipocyte cytokine production. Multiple linear regression analysis showed a model consisting of plasma TNFa and IL-6 predicted the locomotor activity with excellent accuracy, in which mouse activity could be predicted with a linear combination of plasma TNFα and IL6 levels with an R2 of 84% (Figure 5). In addition to these functional effects, marked changes were also noted with the western diet, and again, adipocyte NaKtide treatment ameliorated these, which included protein carbonylation, expression of PSD95 and activation of Tau. The implications of these observations to cognitive and emotional disturbances associated with obesity and other neurodegenerative disorders including aging related cognitive impairment have yet to be explored. We also note that virtually all consequences of obesity such as dyslipidemia and insulin resistance were also attenuated by adipocyte NaKtide expression.

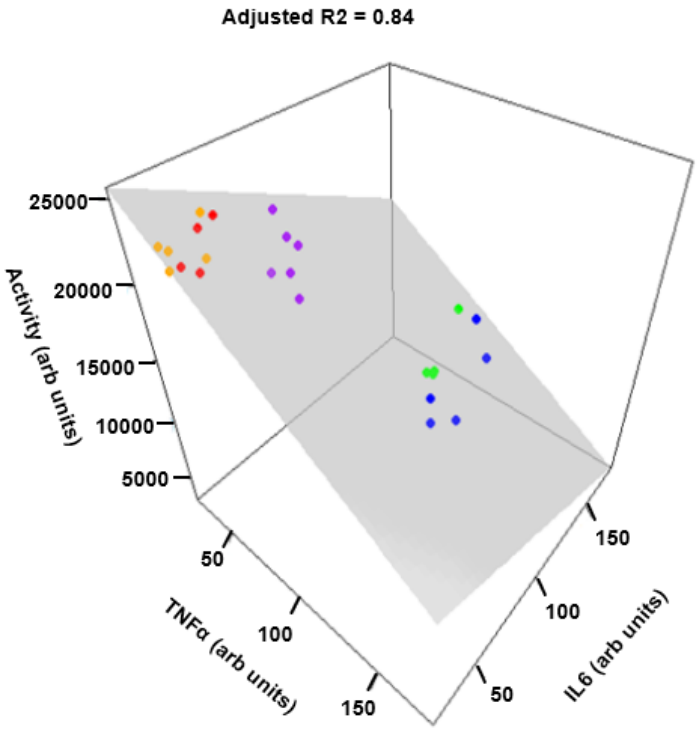

Figure 5: Multiple linear regression analysis between the plasma inflammatory cytokines, IL-6 and TNF-α, predicting the locomotor activity.

Together, our results suggest a central role for the Na/K-ATPase oxidant amplification loop within adipocytes in the pathogenesis of obesity induced by a WD as well as the commonly associated comorbidities. The behavioral changes could be attributed to this deranged adipocyte metabolism which, in turn, were very strongly associated with the levels of cytokines known to be produced by adipocytes. It appears not only that targeting the Na/K-ATPase oxidant amplification loop may be promising in terms of efficacy

as well as limiting off-target effects. If these findings can be confirmed in humans, a number of therapeutic strategies might be envisioned ranging from surgical control of fat mass, molecular biological strategies described in this report to simple dietary manipulations.

Materials and Methods

Experimental Design

All animal studies were approved by the Marshall University Animal Care and Use Committee in accordance with the National Institutes of Health (NIH) Guide for Care and Use of Laboratory Animals. C57BL6 mice (Male, 8 weeks) were purchased from Hilltop Lab Animals. After arriving at the Robert C. Byrd Biotechnology Science Center Animal Resource Facility (ARF) mice were placed in cages and fed a normal chow diet with ad libitum access to water. Animals were randomly divided into five groups as follows: group 1, Control (normal chow); group 2, Adipo-NaKtide (normal chow+ lenti-adiponectin-GFP-NaKtide); group 3, Western Diet (WD); group 4, WD+Adipo-GFP (WD+lenti-adiponectin-GFP); and group 5, WD+Adipo-NaKtide (WD + lenti-adiponectin-GFP-NaKtide). WD was purchased commercially from Envigo (Indianapolis, IN), and contained 42% fat, 42.7% carbohydrate, and 15.2% protein, yielding 4.5 KJ/g specific energy. Fructose was purchased commercially from Alfa Aesar (Ward Hill, MA). Fructose water was made at a concentration of 42g/L, yielding 0.168 KJ/mL of specific energy. Mice in the WD group were given WD and ad libitum access to fructose water.

Lentiviral construct with NaKtide driven by an adiponectin promoter were constructed by Vector Builder Inc. and were used in mice to achieve NaKtide expression specifically in adipose tissue. Lentiviral construct featured the adiponectin promoter driving expression of the NaKtide cassette linked by means of a 2A peptide to eGFP for bicistronic expression (Figure S1). The NaKtide sequence used for this vector was ATGAGCGCCACCTGGCTG-GCCCTGAGCAGGATCGCCGGTCTTTGCAACAGGGCCGT-GTTCCAG. Lentivirus (100 uL, 2X109 TU/mL in saline) with Lenti-GFP-NaKtide and its counterpart Lenti-GFP (driven by adiponectin promoter without NaKtide) were injected into mice intraperitoneally (IP) at week 0. Groups 2 and 5 received an injection of lenti-adiponectin-GFP-NaKtide, and group 4 was given an injection of lenti-adiponectin-GFP as a control of lenti-viral construct. Body weight, food, and water intake were measured weekly for 12 weeks. At the time of sacrifice, the body weight, visceral and subcutaneous fat weight, liver weight, and heart weight were measured. Blood samples were collected for determination of leptin and inflammatory cytokine levels. Tissues were flash frozen in liquid nitrogen and maintained at -80°C, or placed in paraformaldehyde for paraffin embedding.

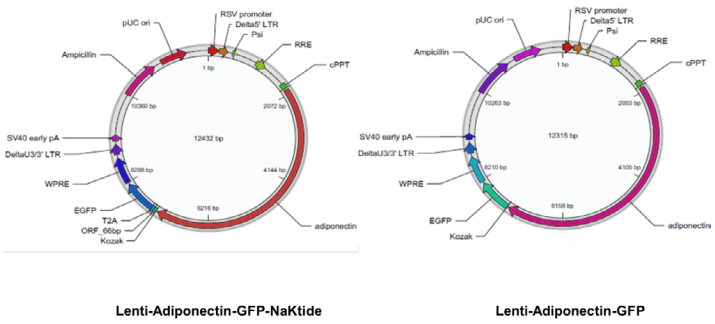

Figure S1: Lentiviral construct of lenti-adiponectin-GFP-NaKtide. An adiponectin promoter drove expression of the NaKtide cassette linked by means of a 2A peptide to eGFP for bicistronic expression.

Indirect calorimetry and locomotor activity

At the end of the 12-week experimental period, energy expenditure and locomotor activity were measured using an eight-chamber CLAM (Columbus Instruments, Columbus, OH, USA). In this system, total oxygen consumption (VO2) and carbon dioxide production (VCO2) were measured, and VO2 was converted to individual heat production (kcal/hour) by Columbus software. This software calculates the heat production by multiplying the calorific value CV=3.815 + (1.232×RER) by the observed VO2 (Heat=CV×VO2). The energy expenditure is then calculated as a ratio of heat produced divided by body mass. A system of infrared beams detects movement of animals in CLAMS, and locomotor activity was determined as ambulatory count, the number of times different beams were broken in either the x- or y-axes during an interval. All mice were acclimatized to the cages for 24 hours prior to an additional 48 hours of recordings under the regular 12- hour light/dark cycle.

Glucose Tolerance Test

At the end of the 12-week period, mice were fasted for 8 hours. After the fasting period, a 10% glucose solution (2g/kg body weight) was injected intraperitoneally. Samples were taken from the tail vein at 0, 30, 60, 90, and 120 minutes after glucose injection. Blood glucose was measured using the Accutrend Sensor glucometer.

Cytokine and Leptin Measurements

Plasma levels of TNFα, IL-6, MCP-1, and leptin were measured using ELISA assay kits according to manufacturer instructions (Abcam Cambridge, MA).

RNA extraction and real time PCR

Total RNA was extracted from adipose tissue using RNeasy Protect Mini Kit (QIAGEN, Maryland) per manufacture's instruction. Total RNA was analyzed by a quantitative real time polymerase

chain reaction. Real time PCR was done using SYBR Green PCR Master Mix on a 7500 HT Fast Real-Time PCR System (Applied Biosystems, US). Each reaction was done in triplicate. All experimental samples were normalized using GAPDH. Specific primers were used for MFN 1 and 2, Sirt3, TNFα, and Leptin.

Western Blot Analysis

Visceral adipose tissue and brain tissue were pulverized with liquid nitrogen and placed in RIPA homogenization buffer with protease inhibitor cocktail. Homogenates were centrifuged, the supernatant was isolated, and immunoblotting performed. Adipose tissue was used for determination of α1 and α2 subunits of the Na/K-ATPase, FAS, PPARγ, MEST, and PGC1α. Antibodies were from Millipore-Sigma (Burlington, MA) for detection of α1 and α2 subunits, from Cell Signaling (Danvers, MA) for detection of FAS and PPARγ, and from Abcam (Cambridge, MA) for detection of MEST and PGC1α.

Brain tissue was used for expression of tyrosine hydroxylase (TH), PSD95, p-Tau, and Tau expression. Antibody against TH was from Abcam (Cambridge, MA), and antibodies against PSD95, p-Tau, and Tau were from Cell Signaling (Danvers, MA).

Measurement of c-Src phosphorylation was performed with whole cell lysates from visceral adipose tissue that were prepared with RIPA buffer with protease inhibitor cocktail. Activation of c-Src was determined as described previously [19]. Polyclonal anti-Src [pY418] phospho-specific antibody was from Invitrogen (Camarillo, CA). Monoclonal antibody against total c-Src was from Santa Cruz (Santa Cruz, CA). After immunoblotting for phospho-Src, the same membrane was stripped and blotted for total c-Src. Activation of c-Src was expressed as the ratio of phospho-Src/c-Src with measurements normalized to 1 for control samples.

Assessment of protein carbonylation was performed with whole cell lysates from visceral adipose tissue and brain tissue were prepared with RIPA buffer with protease inhibitor cocktail and western blotting for protein carbonylation assay was done as previously described [19]. 2, 4-dinitrophenylhydrazine (DNPH) and antibody against 2, 4-dinitrophenyl (DNP) hydrazone derivatives were purchased from Sigma-Aldrich. The signal density values of control samples were normalized to 1 with Coomassie blue staining.

For western immunoblotting analysis, each gel included two samples from each experimental group. The first control sample's value of each gel was set as 1.0, all other samples in the same gel were compared to this first control sample. In Figures or Figure Legends, all the n numbers indicated independent biological samples.

Hematoxylin and Eosin Staining

Visceral adipose tissue was cut into 6 μm sections and stained with hematoxylin and eosin for histological analysis. Adipocyte number and area was determined using ImageJ software (NIH) as described [47]. In brief, H&E-stained adipose tissue images (20X magnification) were opened in ImageJ. Images were changed to 8 bit, enhanced through Threshold, Dilate, and Watershed functions, converted to mask using the binary function, and enhanced. Black and white images were compared to the original image to ensure accurate representation of adipocytes. The total number and size of adipocytes was calculated using the "analyze particles" command. To calculate the number of adipocytes, the size of the sample was normalized based on the number of pixels present in the image and the magnification. This was consistently used for all subsequent images. The number of total adipocytes in the distribution is calculated from this for scale.

Statistical analyses

The plots used were combination of scatter and boxplots. The boxplot displays the distribution of the data. It visualizes five summary statistics (the median, two hinges and two whiskers), and all "outlying" points individually [48]. The boxplot was defined by:

Notch lower = median - 1.58 * interquartile range (IQR) / sqrt (n) [49]

Middle = median

Notch upper = median + 1.58 * IQR / sqrt (n);

Lower hinge is the 25th percentile

Upper hinge is the 75th percentile

Data were analyzed and presented with the statistical program R using the packages ggplot2 and doBy. Multiple groups of parametric data (passed Shapiro-Wilk normality test) were compared with one way analysis of variance (ANOVA) and individual group means compared with an unpaired t-test employing the Holm correction for multiple comparisons. Nonparametric data were analyzed with the Wilcoxon rank sum test, also employing the Holm correction for multiple comparisons. All data comparisons are presented at the NS, $p<0.05$ and $p<0.01$ levels. The fit of a plane based on TNFa and IL6 to locomotion was performed using linear regression and displayed with the R package plot3D.

Acknowledgements

This work was supported by National Institutes of Health Grants HL109015 (to J.I.S. and Z.X.), HL071556 and HL105649 (to J.I.S.), NHLBI 223054 (to J.L.), by the Brickstreet Foundation (to J.I.S.) and by the Huntington Foundation, Inc. We also

acknowledged Paul Jones from the Cabell Huntington Hospital Pathology department for his help in the processing of tissues for histological examination.

Authors Contributions

Rebecca D. Pratt: Performed the experiments and participated in the writing of the manuscript

Cameron Brickman: Performed the experiments

Athar Nawab: Performed the experiments

Cameron Cottrill: Performed the experiments

Brian Snoad: Performed the experiments

Hari Vishal Lakhani: Performed the experiments

Juan R. Sanabria: Edited the manuscript

Komal Sodhi: Designed the experiments and edited the manuscript

Zijian Xie: Designed the experiments

Joseph I. Shapiro: Designed the experiments, analyzed data, and wrote the manuscript

Jiang Liu: Designed the experiments and wrote the manuscript

Competing Interests: All the authors declare that there are no competing interests.

References

1. Pugazhenthi S, Qin L, Reddy PH (2017) Common neurodegenerative pathways in obesity, diabetes, and Alzheimer's disease. Biochim Biophys Acta Mol Basis Dis, 1863:1037-1045.
2. Hruby A, Hu FB (2015) The Epidemiology of Obesity: A Big Picture. Pharmacoeconomics, 33: 673-689.
3. Cui H, Kong Y, Zhang H (2012) Oxidative stress, mitochondrial dysfunction, and aging. J Signal Transduct, 2012: 646354.
4. Oberg BP, McMenamin E, Lucas FL, McMonagle E, Morrow J, et al. (2004) Increased prevalence of oxidant stress and inflammation in patients with moderate to severe chronic kidney disease. Kidney Int, 65: 1009-1016.
5. Xie Z, Askari A (2002) Na(+)/K(+)-ATPase as a signal transducer. Eur J Biochem, 269: 2434-2439.
6. Xie Z, Cai T (2003) Na+-K+--ATPase-mediated signal transduction: from protein interaction to cellular function. Mol Interv, 3: 157-168.
7. Xie Z, Xie J (2005) The Na/K-ATPase-mediated signal transduction as a target for new drug development. Front Biosci, 10: 3100-3109.
8. Aperia A (2007) New roles for an old enzyme: Na,K-ATPase emerges as an interesting drug target. J Intern Med, 261: 44-52.
9. Liu J, Xie ZJ (2010) The sodium pump and cardiotonic steroids-induced signal transduction protein kinases and calcium-signaling microdomain in regulation of transporter trafficking. Biochim Biophys Acta, 1802: 1237-1245.
10. Li Z, Xie Z (2009) The Na/K-ATPase/Src complex and cardiotonic steroid-activated protein kinase cascades. Pflugers Arch, 457: 635-644.
11. Tian J, Cai T, Yuan Z, Wang H, Liu L, et al. (2006) Binding of Src to Na+/K+-ATPase forms a functional signaling complex. Mol Biol Cell, 17: 317-326.
12. Liang M, Cai T, Tian J, Qu W, Xie ZJ (2006) Functional Characterization of Src-interacting Na/K-ATPase Using RNA Interference Assay. J Biol Chem, 281: 19709-19719.
13. Bagrov AY, Shapiro JI (2008) Endogenous digitalis: pathophysiologic roles and therapeutic applications. Nat Clin Pract Nephrol, 4:378-392.
14. Bagrov AY, Shapiro JI, Fedorova OV (2009) Endogenous cardiotonic steroids: physiology, pharmacology, and novel therapeutic targets. Pharmacol Rev, 61: 9-38.
15. Pierre SV, Xie Z (2006) The Na,K-ATPase receptor complex: its organization and membership. Cell Biochem Biophys, 46: 303-316.
16. Liu J, Tian J, Chaudhry M, Maxwell K, Yan Y, et al. (2016) Attenuation of Na/K-ATPase Mediated Oxidant Amplification with pNaKtide Ameliorates Experimental Uremic Cardiomyopathy. Sci Rep, 6: 34592.
17. Drummond CA, Fan X, Haller ST, Kennedy DJ, Liu J, et al. (2018) Na/K-ATPase signaling mediates miR-29b-3p regulation and cardiac fibrosis formation in mice with chronic kidney disease. PLoS One, 13: e0197688.
18. Drummond CA, Hill MC, Shi H, Fan X, Xie JX, et al. (2016) Na/K-ATPase signaling regulates collagen synthesis through microRNA-29b-3p in cardiac fibroblasts. Physiol Genomics, 48: 220-229.
19. YanY, Shapiro AP, Haller S, Katragadda V, Liu L, et al. (2013) Involvement of reactive oxygen species in a feed-forward mechanism of Na/K-ATPase-mediated signaling transduction. J Biol Chem, 288: 34249-58.
20. Wang Y, Ye Q, Liu C, Xie JX, Yan Y, et al. (2014) Involvement of Na/K-ATPase in hydrogen peroxide-induced activation of the Src/ERK pathway in LLC-PK1 cells. Free Radic Biol Med, 71:415-426.
21. Li Z, Cai T, Tian J, Xie JX, Zhao X, et al. (2009) NaKtide, a Na/K-ATPase-derived peptide Src inhibitor, antagonizes ouabain-activated signal transduction in cultured cells. J Biol Chem, 284: 21066-21076.
22. Wu W, Zhang J, Zhao C, Sun Y, Yin Y, et al. (2018) Lentivirus-mediated CTRP6 silencing ameliorates diet-induced obesity in mice. Exp Cell Res, 367: 15-23.
23. Eerola K, Nordlund W, Virtanen S, Dickens AM, Mattila M, et al. (2013) Lentivirus-mediated alpha-melanocyte-stimulating hormone overexpression in the hypothalamus decreases diet induced obesity in mice. J Neuroendocrinol, 25: 1298-1307.
24. Bian J, Bai XM, Zhao YL, Zhang L, Liu ZJ (2013) Lentiviral vector-mediated knockdown of Lrb in the arcuate nucleus promotes diet-induced obesity in rats. J Mol Endocrinol, 51: 27-35.
25. Ames RS, Lu Q (2009) Viral-mediated gene delivery for cell-based assays in drug discovery. Expert Opin Drug Discov, 4: 243-256.
26. Massiera F, Seydoux J, Geloen A, Quignard-Boulange A, Turban S, et al. (2001) Angiotensinogen-deficient mice exhibit impairment of diet-induced weight gain with alteration in adipose tissue development and increased locomotor activity. Endocrinology, 142: 5220-5225.
27. Dubey L, Hesong Z (2006) Role of leptin in atherogenesis. Exp Clin Cardiol, 11: 269-275.
28. Fernandez-Sanchez A, Madrigal-Santillan E, Bautista M, Esquivel-Soto J, Morales-González A, et al. (2011) Inflammation, oxidative

stress, and obesity. Int J Mol Sci, 12: 3117-3132.

29. Bartlett DE, Miller RB, Thiesfeldt S, Lakhani HV, Shapiro JI, et al. (2018) The Role of Na/K-ATPase Signaling in Oxidative Stress Related to Aging: Implications in Obesity and Cardiovascular Disease. Int J Mol Sci, 19:2139.

30. Dalle-Donne I, Rossi R, Giustarini D, Milzani A, Colombo R (2003) Protein carbonyl groups as biomarkers of oxidative stress. Clin Chim Acta, 329: 23-38.

31. Daubner SC, Le T, Wang S (2011) Tyrosine hydroxylase and regulation of dopamine synthesis. Arch Biochem Biophys, 508:1-12.

32. Mundorf ML, Joseph JD, Austin CM, Caron MG, Wightman RM (2001) Catecholamine release and uptake in the mouse prefrontal cortex. J Neurochem, 79: 130-142.

33. Kothari V, Luo Y, Tornabene T, O'Neill AM, Greene MW, et al. (2017) High fat diet induces brain insulin resistance and cognitive impairment in mice. Biochim Biophys Acta Mol Basis Dis, 1863: 499-508.

34. Boudina S, Graham TE (2014) Mitochondrial function/dysfunction in white adipose tissue. Exp Physiol, 99: 1168-1178.

35. Villena JA (2015) New insights into PGC-1 coactivators: redefining their role in the regulation of mitochondrial function and beyond. FEBS J, 282: 647-672.

36. Yan Y, Shapiro AP, Mopidevi BB, Chaudhry MA, Maxwell K, et al. (2016) Protein Carbonylation of an Amino Acid Residue of the Na/K-ATPase alpha1 Subunit Determines Na/K-ATPase Signaling and Sodium Transport in Renal Proximal Tubular Cells. J Am Heart Assoc, 5: e003675.

37. Liu J, Kesiry R, Periyasamy SM, Malhotra D, Xie Z, et al. (2004) Ouabain induces endocytosis of plasmalemmal Na/K-ATPase in LLC-PK1 cells by a clathrin-dependent mechanism. Kidney Int, 66: 227-241.

38. Cai H, Wu L, Qu W, Malhotra D, Xie Z, et al. (2008) Regulation of apical NHE3 trafficking by ouabain-induced activation of the basolateral Na+-K+-ATPase receptor complex. Am J Physiol Cell Physiol, 2008. 294: C555-C563.

39. Huang WH, Wang Y, Askari A, Zolotarjova N, Ganjeizadeh M (1994) Different sensitivities of the Na+/K(+)-ATPase isoforms to oxidants. Biochim Biophys Acta, 1190: 108-114.

40. Huang WH, Wang Y, Askari A (1992) (Na+ + K+)-ATPase: inactivation and degradation induced by oxygen radicals. Int J Biochem, 24: 621-626.

41. Thevenod F, Friedmann JM (1999) Cadmium-mediated oxidative stress in kidney proximal tubule cells induces degradation of Na+/K(+)-ATPase through proteasomal and endo-/lysosomal proteolytic pathways. FASEB J, 13: 1751-1761.

42. Liu J, Kennedy DJ, Yan Y, Shapiro JI (2012) Reactive Oxygen Species Modulation of Na/K-ATPase Regulates Fibrosis and Renal Proximal Tubular Sodium Handling. Int J Nephrol, 2012: 381320.

43. Kim MS, Akera T (1987) O2 free radicals: cause of ischemia-reperfusion injury to cardiac Na+-K+-ATPase. Am J Physiol, 252: H252-7.

44. Furukawa S, Fujita T, Shimabukuro M, Iwaki M, Yamada Y, et al. (2004) Increased oxidative stress in obesity and its impact on metabolic syndrome. J Clin Invest, 114: 1752-1761.

45. Le Lay S, Simard G, Martinez MC, Andriantsitohaina R (2014) Oxidative stress and metabolic pathologies: from an adipocentric point of view. Oxid Med Cell Longev, 2014: 908539.

46. Vincent HK, Taylor AG (2006) Biomarkers and potential mechanisms of obesity-induced oxidant stress in humans. Int J Obes (Lond), 30: 400-418.

47. Parlee SD, Lentz SI, Mori H, MacDougald OM (2014) Quantifying size and number of adipocytes in adipose tissue. Methods Enzymol, 537: 93-122.

48. van Raalte H, Egorov V (2015) Tactile Imaging Markers to Characterize Female Pelvic Floor Conditions. Open J Obstet Gynecol, 5: 505-515.

49. Stolarczyk A, Horvath A, Szczechura M, Kamińska M, Dziechciarz P (2014) High prevalence of vitamin D insufficiency in community-dwelling postmenopausal Polish women. Prz Menopauzalny, 13:289-292.